Catal Lett (2007) 118:118–122
DOI 10.1007/s10562-007-9161-2

CO Oxidation on Anatase TiO_2 Nanotubes Array and the Effect of Defects

S. Funk · Uwe Burghaus

Received: 24 May 2007 / Accepted: 7 June 2007 / Published online: 28 July 2007

Abstract The adsorption of O_2 and the CO oxidation reaction has been studied, by TDS and surface titrations, on a TiO_2 nanotubes (TiNTs) array which consist of a 80/20% mixture of the anatase/rutile polymorph. Molecular O_2 adsorption, influenced by defects, as well as CO_2 formation at low temperatures (~100 K) were observed.

Keywords Gas surface interactions · Adsorption kinetics · Thermal desorption spectroscopy · Anatase · Rutile · TiO_2 nanotubes

1 Introduction

A kinetics study about oxygen adsorption and CO oxidation on a TiO_2 nanotubes array (TiNT) at low temperatures is presented. The CO oxidation reaction is one of the most important prototypes of bimolecular surface reactions. Triggered by the recent discovery of the nano-Au TiO_2catalyst [1, 2], the low temperature CO oxidation reaction has again attracted significant interest [3–5]. Besides the cleaning of exhaust pollution, the removal of CO from syngas is required for (low temperature) fuel cell catalysts, since trace amounts of CO can poison the surface of fuel cell electrodes [6]. Furthermore, a number of more exotic but important applications exist such as closed-cycle CO_2 lasers [7], which require low temperature CO oxidation catalysts. TiO_2 is particular attractive due to its unique photocatalytic properties [8, 9] which could, combined with capture effects [10–14] of nanotubes, lead to significantly enhanced catalytic activity of TiNTs. Already quite diverse applications of TiNTs are reported in materials science [15], medicine [16], and catalysis [17]. Although TiO_2 exists in different crystallographic phases, most surface science studies have focused on rutile TiO_2(110) [18]. However, industrial TiO_2 powder catalysts consist of rutile and anatase crystallites. It has been proposed [8, 19] that the most catalytically active polymorph is anatase. Therefore, studies on the anatase polymorph appear pertinent. TiO_2 nanotubes and nanoparticles are, due to their smaller surface energy [20], intrinsically of the anatase polymorph [21–23]. Annealing procedures can lead to mixed anatase/rutile TiO_2 nanotubes.

In this letter we present evidence for CO oxidation on TiNTs by molecularly adsorbed oxygen. Furthermore, TDS experiments reveal different adsorption states of oxygen dosed at low temperatures on TiNTs. Experiments devoted to the effect of crystal structure of TiNTs have been presented elsewere [22].

2 Materials and Experimental Procedures

A TiO_2 nanotubes array (TiNT) sample has been obtained from P. Schmuki's group at Erlangen-Nuernberg University (Germany). The synthesis procedures are detailed in Ref. [24, 25]. The sample has been characterized by X-ray diffraction (XRD) which revealed that the tubular structure of the open-ended TiO_2 nanotubes consists of a 80/20% mixture of anatase/rutile crystallites; for details see Ref. [22]. X-ray photoelectron spectroscopy revealed, as the only impurity, carbon close to the detection limit [26]. The sample has been degassed in ultra-high vacuum by annealing at 500–600 K [22]. Scanning electron microscopy data (SEM) as well as XRD collected after

S. Funk · U. Burghaus (✉)
Department of Chemistry, North Dakota State University, Fargo, ND, USA
e-mail: uwe.burghaus@ndsu.edu

the kinetics experiments revealed that no modification in the sample's morphology occurred. The TDS set up is detailed in Ref. [27]; a line-of-sight detection with a shielded mass spectrometer (see inset of Fig. 3) has been used. Oxygen has been dosed by backfilling. An exponential background was removed from each TDS curve and the data have been smoothed conserving, however, the shape of the curves. The reading of the thermocouple has been calibrated (±5 K) in situ by TDS using the known heat of condensation of alkanes. A heating rate of 1 K/sec has been used for all TDS measurements; the exposures are given in Langmuir (1 L equals 1 s gas exposure at 1×10^{-6} torr). He gas was fluxed through the liquid nitrogen containing sample holder rod to further reduce the sample temperature [28].

3 Data Presentation and Discussion

Figure 1 depicts a set of TDS curve s for oxygen adsorbed at ~100 K on the anatase/rutile mixed TiNT sample. Two structures are evident. A low temperature peak (α_1) which shifts from 129 K to 115 K with increasing exposure and a second broad structure (α_2) centered at about 200 K. The low desorption temperatures suggest that the α_1 peak corresponds to a molecular adsorption/desorption pathway of O_2. Molecular O_2 adsorption has been observed for TiO_2(110) as well as supported TiO_2(110) [4, 29]. (We may add that the desorption of oxygen was below the detection limit of the mass spectrometer for adsorption temperatures above 300 K and no desorption of O_2 has been observed from the back side of the sample at low adsorption temperatures which could be assigned to the α_1 or α_2 TDS peaks.) However, the shift of the α_1 peak indicates either deviations from 1st-order kinetics which have been observed in some cases for molecular adsorption on metal catalysts [30] or coverage dependent kinetics. The most plausible explanation for deviations from 1st-order kinetics are structural effects such as desorption starting along the rim of islands of the adsorbates or along the rim of the crystallites which constitute the tubular structure of the nanotubes.

Interestingly, the α_2 peak intensity depends distinctly on the sample's history (Fig. 1(II)). While collecting this set of TDS data, the sample has not been flashed above 300 K and the experiment started with collecting the curves at low exposures. Thus, while the initial exposure increased from 1 L to 240 L the total amount of oxygen dosed on the surface also increased and the α_2 TDS peak intensity decreased. Although we cannot rule out a stabilization of molecular oxygen on or at the vicinity of defect sites, the quenching of the α_2 peak strongly suggests dissociative oxygen adsorption on defect sites. The formed oxygen

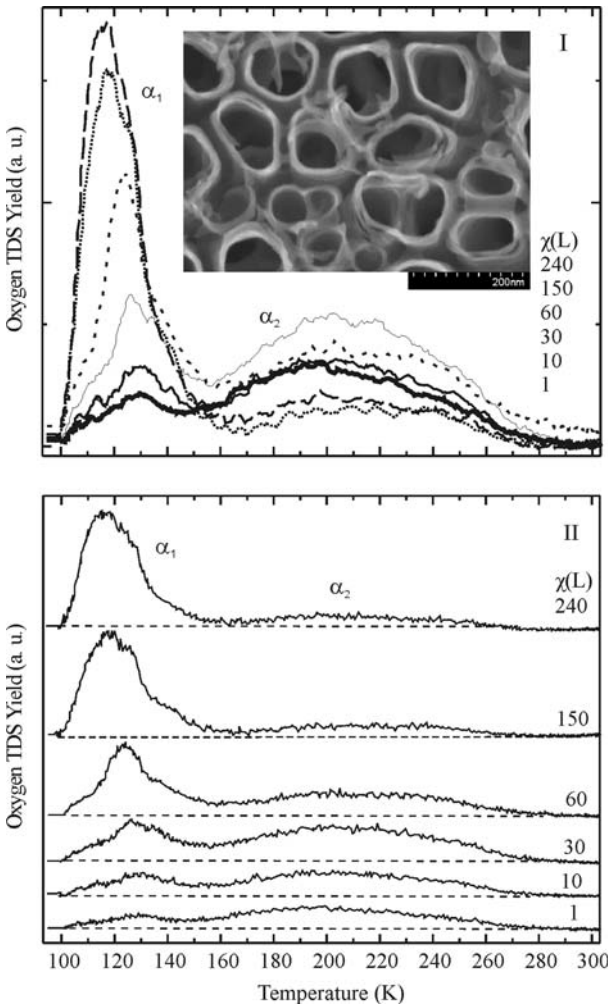

Fig. 1 Thermal desorption spectroscopy curves for O_2 adsorption at 100 K on TiO_2 nanotubes as a function of exposure. (**I**) The curves are plotted one over the other allowing for an intensity comparison and (**II**) the same curves are offset to reveal the variations in the TDS peak intensities. (The data in panel I are smoothed, those in panel II are not.) The inset shows a scanning electron microscopy image of a typical TiNT sample

atoms "heal out" defects, the better the more oxygen has been dosed on the surface. The remaining oxygen atoms desorb recombinatively (α_2 peak). The symmetric shape of the α_2 TDS is also consistent with recombinative desorption. Related effects have been reported for rutile TiO_2(110) single crystals [31]. This process is typically observed at greater surface temperatures due to larger binding energies of atomically bonded as compared with molecularly bonded oxygen. The rather large width of the α_2 TDS peak suggests, however, differences in the local adsorption geometry such as adsorption on multiple defect sites, defects at the edge of the crystallites, and on terrace sites. Furthermore, the TiNT sample consists of anatase and rutile crystallites. Thus, different defect sites and slight variations in binding energies of adsorbed oxygen are

expected from the complicated tubular structure of the TiNTs which consists of a large amount of structural defects as evident from SEM results [22]. Therefore, a large width of the α_2 TDS peak is expected. Besides the larger variation in the Arrhenius factor at lower adsorption temperatures, the nondissociative adsorption of molecular oxygen would be restricted to more homogeneous sites ("pristine sites") leading to a smaller width of the α_1 peak. In order to verify the origin of the high-temperature TDS peak, several test experiments have been conducted which are discussed below, see Figs. 2 and 3.

Figure 2 summarizes the results of cycles of O_2 adsorption/desorption experiments. Two sets of identical experiments are shown (see panel I and II). Before the start of the experiments, the sample has been annealed in vacuum at 550–600 K for 3 min. The first O_2 TDS experiment (cycle #1) shows a very distinct α_2 peak. Repeating now adsorption/desorption cycles within the temperature rage of

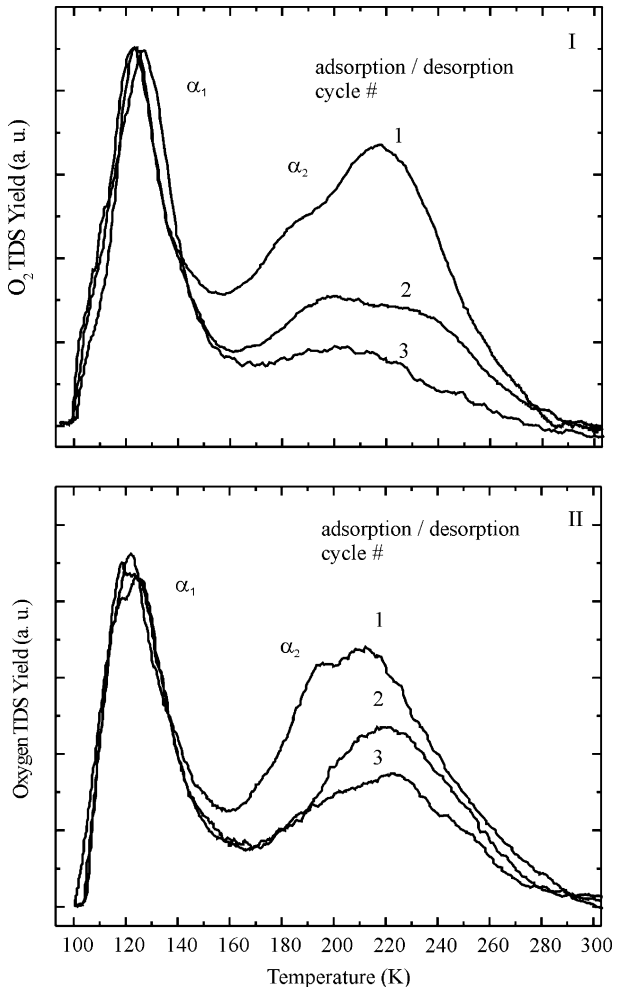

Fig. 2 The filing (healing out) of oxygen vacancy sites is evident from O_2 adsorption/desorption cycles monitored by TDS. Two sets of experiments where 60 L of oxygen have been adsorbed at 100 K are shown

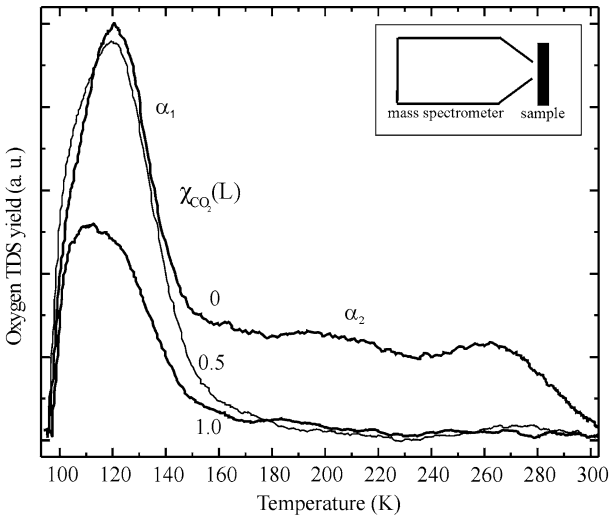

Fig. 3 Coadsorption experiments of CO_2 and oxygen. χ_{CO2} Langmuir (L) of CO_2 has been dosed first on the surface which leads to blocking of defect sites. Afterwards, 60 L of oxygen have been exposed and an O_2 TDS curve has been collected. (The inset shows the TDS set up used for all experiments.)

100–300 K (three cycles, #1–#3, are shown in each panel) leads to a decrease of the α_2 peak intensity with respect to the α_1 TDS peak intensity (Fig. 2(I)). This behavior was well reproducible after annealing the sample again. A second set of data is shown in Fig. 2(II). This result already supports the conclusion that the α_2 peak is related with oxygen vacancy sites on the TiNT surface. An effect of water [32] or hydrogen uptake [33] from the background appears unlikely to be the reason for the quenching of the α_2 TDS peak since this effect was clearly related with the amount of oxygen dosed on the surface. In order to check that the O_2 TDS peaks are indeed related with different adsorption sites, coadsorption experiments with CO_2 have been conducted.

It is well documented that CO_2 is a very useful probe molecule to distinguish pristine and defect sites on metal oxides [34–36]. For rutile TiO_2(110), CO_2 adsorbs initially preferentially on defect sites as the highest binding energy sites. Therefore, dosing CO_2 first and then O_2 should lead to a quenching of the α_2 peak if it is related with different adsorption sites (defects) than the α_1 TDS peak (pristine sites). On the other hand, if the α_2 structure is simply related with a coverage dependence of the adsorption kinetics, the α_2 TDS peak would not be strongly affected by site blocking effects. Indeed, as depicted in Fig. 3, pre-exposing CO_2 at low temperatures reduces predominantly the intensity of the α_2 TDS peak. This result identifies that different adsorption sites are involved in the O_2 adsorption scenario.[1] At larger

[1] CO_2 does not adsorb on the sample holder which consists mostly of steel. Therefore, the coadsorption experiments also rule out artifacts from the sample holder in the TDS experiments.

exposures CO_2 will certainly also occupy pristine sites and the α_1 TDS peak intensity also decreases.

As an application in catalysis and as another test that kinetically distinct oxygen species form on the TiNTs, leak valve CO titration experiments [37, 38] have been conducted for TiNTs precovered with oxygen at low temperatures (see Fig. 4). Figure 4(I) shows in the upper section the CO_2 formation as a function of CO exposure time. The CO pressure has been increased step-like (see lower section in Fig. 4(I)) which defines the zero point on the reaction time scale. Two experimental runs, conducted at different reaction temperatures, are shown. The lower reaction temperature leads to a faster decay of the CO_2 signal. Thus, the reaction kinetics are characterized by a negative apparent activation energy [39], i.e., the CO_2 product formation is limited by the CO coverage on the surface. Due to the small binding energies of CO, its coverage decreases rapidly with increasing temperature which leads to an acceleration of the kinetics with decreasing reaction temperature for bimolecular reactions. This type of kinetics ("faster reactions at lower reaction temperatures") is common for low temperature CO oxidation catalysts. Related results have been obtained for silver[38, 39], gold [40], and copper [41, 42] single crystals. Conducting post-reactive O_2 TDS experiments verifies that indeed oxygen has been titrated by CO from the surface (Fig. 4(II)). Interestingly, the molecular oxygen species (α_1 peak) appear to be more reactive towards CO_2 formation at low temperatures than atomically bonded oxygen (α_2 peak). CO oxidation by molecularly bonded oxygen has been observed for silver single crystals [37, 43, 44]. In the case of Ag(110), the formation of a O_2–CO_2 intermediate had been postulated [37, 38] by kinetics experiments and verified later by a time resolved scanning tunneling microscopy study [45]. Independent of the mechanism, the different CO_2 formation rates which are related to the α_1 and α_2 TDS features indicate again that different oxygen species and adsorption sites are involved.

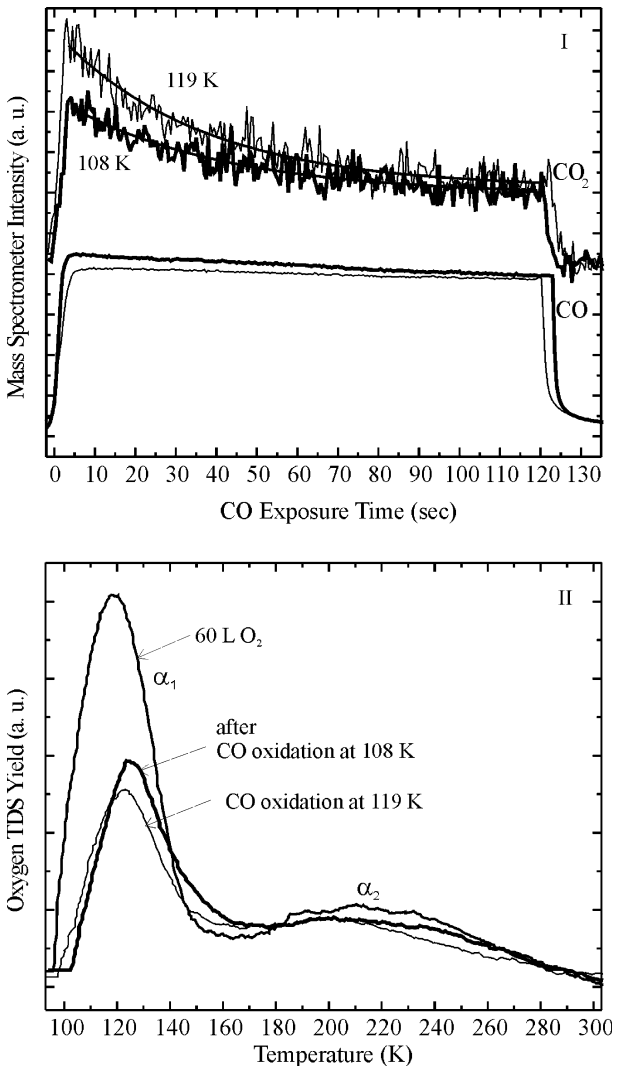

Fig. 4 CO titration experiments of oxygen adsorbed at low temperatures on a TiO_2 nanotubes array. (**I**) CO_2 formation for two different reaction temperatures as well as the CO pressure in the reaction chamber as a function of time. The CO_2 signal can for 108 K be fitted with exp(-time/39) and the one for 119 K with exp(-time/35). (**II**) O_2 TDS after the titration experiments as compared with an O_2 TDS blind experiment. (60 L O_2 at 100 K, titration with 1×10^{-6} torr of CO)

4 Summary and Conclusions

The experimental evidence strongly suggests that oxygen molecules dissociate on oxygen vacancy sites, as they do on TiO_2 single crystals, filling defect and adjacent pristine sites on the TiNTs. The oxygen atoms adsorbed on pristine sites can be flashed off resulting in the α_2 TDS peak (recombinative oxygen desorption). The remaining oxygen atoms fill the oxygen vacancy sites leading to a quenching of this adsorption pathway in subsequent O_2 adsorption/desorption cycles. Molecular adsorption on defect sites may be possible but would not explain the observed quenching of the α_2 TDS peak. Annealing of the TiNTs in UHV to higher temperatures restores the α_2 adsorption pathway, indicating that surface oxygen (which is part of the TiO_2 crystal lattice) desorption is a slow process with larger activation energy. As a parallel adsorption pathway oxygen adsorbs molecularly on pristine sites leading to the α_1 TDS structure. The pristine sites have been identified as fivefold coordinated Ti^{4+} sites for TiO_2 single crystals and defect sites as Ti^{3+} oxygen vacancy sites [29, 31]. These sites must also exist on TiO_2 nanotubes in addition to more complicated defects such as the grain boundaries of the crystallites. Despite some similarities of TiO_2 single crystals and TiNTs major differences in the adsorption kinetics

of oxygen exists. For example, oxygen does not adsorb on fully oxidized rutile TiO_2(110) [29]. The TiNTs, which are polycrystalline and mostly of the anatase polymorph are intrinsically active toward oxygen adsorption [22].

The activity for CO oxidation on clean TiO_2 catalyst is somewhat surprising at a quick glance. However, theoretical studies revealed that a Mars van Krevelen mechanism which involves lattice oxygen would energetically be possible for CO oxidation on an anatase TiO_2 system [46]. The reactivity is related with poorly coordinated oxygen atoms; i.e., with surface defects. A distinct reactivity of defects sites has also been identified theoretically for rutile TiO_2 [47, 48]. On the other hand, catalytic activity of non supported and defect free rutile TiO_2(110) for CO oxidation at low temperatures has also been seen [49]. Certainly further studies are required to determine precisely kinetics parameters as well as spectroscopic studies providing additional evidence for the assignment of the adsorption sites proposed here.

Acknowledgments We gratefully acknowledge the support of P. Schmuki and his group, particularly A. Ghicov, for providing the samples. Financial support by the DoE-EPSCoR (DE-FG02-06ER46292, state grant) and from ND NSF-EPSCoR IIP seed (EPS-047679) is acknowledged.

References

1. Haruta M (1997) Catal Today 36:153
2. Chen MS, Goodman DW (2004) Science 306:252
3. Kim TS, Stiehl JD, Reeves CT, Meyer RJ, Mullins CB (2003) J Am Chem Soc 125:2018
4. Stiehl JD, Kim TS, McClure SM, Mullins CB (2004) J Am Chem Soc 126:1606
5. Stiehl JD, Kim TS, Reeves CT, Meyer RJ, Mullins CB (2004) J Phys Chem 108:7917
6. Larminie J, Dicks A (2003) Wiley, ISBN 0-470-84857-X
7. Gardner SD, Hoflund GB, Schryer DR, Schryer J, Upchurch UT, Kielin EJ (1991) Langmuir 7:2135
8. Thompson TL, Yates JT (2006) Chem Rev 106:4428
9. Henderson MA (2002) Surf Sci Reports 46:1
10. Tenne R (2002) A: Physicochem Eng Aspects 208:83
11. Kondratyuk P, Yates JT (2004) Chem Phys Lett 383:314
12. Funk S, Hokkanen B, Nurkig T, Burghaus U, White B, O'Brien S, Turro N (2007) J Phys Chem C 111:8043
13. Tenne R, Homyonfer M, Feldman Y (1998) Chem Mater 10(11):3225
14. Tenne R (2006) Nat Nanotechnol 1:103
15. Wang H, Yip CT, Cheung KY, Djurisic AB, Xie MH, Leung YH, Chan WK (2006) Appl Phys Lett 89:123
16. Seunghan O, Sungho J (2006) Mater Sci & Eng, C: Biomim Supramol Syst 26:1301
17. Liu X, Jaramillo TF, Kolmakov A, Baeck SH, Moskovits M, Stucky GD, McFarland EW (2005) J Mat Res 20:1093
18. Cox PA (1995) Clarendon Press, Oxford
19. Satterfiled CN (1991) Heterogeneous catalysis in industrial practice. McGraw-Hill, Inc., New York
20. Lazzeri M, Vittadini A, Selloni A (2001) Phys Rev B 63:155409
21. Ghicov A, Macak JM, Tsuchiya H, Kunze J, Haeublein V, Frey L, Schmuki P (2006) Nano Lett 6:L1080
22. Funk S, Hokkanen B, Burghaus U, Ghicov A, Schmuki P (2007) Nano Lett 7:1091
23. Bing Z, Hermans S, Somorjai GA (eds) (2004) Nanotechnology in catalysis, springer series: nanostructure science and technology, ISBN 0-306-48323–8
24. Macak JM,Tsuchiya H,Taveira L, Aldabergerova S, Schmuki P (2005) Angewandte Chemie International Edition 44:7463–7465
25 Ghicov A, Tsuchiya H, Macak JM, Schmuki P (2006) Physica Status Solidi A: Appl Mater Sci 203:R28
26. Funk S, Hokkanen B, Nurkic T, Goering J, Kadossov E, Burghaus U, Ghicov A, Schmuki P, Yu ZQ, Thevuthasan S, Saraf LV (2007) In: ACS-Chicago conference proceedings
27. Wang J, Hokkanen B, Burghaus U (2005) Surf Sci 577:158
28. Yates JT (1988) New York, AIP Press Springer
29. Henderson MA, Epling WS, Perkins CL, Peden CH, Diebold U (1999) J Phys Chem B 103:5328
30. Vollmer M, Träger F (1987) Surf Sci 187:445
31. Epling WS, Peden CHF, Henderson MA, Diebold U (1998) Surf Sci 412/413:333
32. Herman GS, Dohnalek Z, Ruzycki N, Diebold U (2003) J Phys Chem B 107:2788
33. Staemmler V, Fink K, Meyer B, Marx D, Kunat M, Gil Girol S, Burghaus U, Wöll Ch (2003) Phys Rev Lett 90:106102
34. Henderson MA (1998) Surf Sci 400:203
35. Thompson TL, Diwald O, Yates JT (2003) J Phys Chem 107:11700
36. Funk S, Burghaus U (2006) Phys Chem Chem Phys 8:4805
37. Burghaus U, Conrad H (1996) Surf Sci 364:109
38. Burghaus U, Conrad H (1997) Surf Sci 370:17
39. Burghaus U, Conrad H (1995) Surf Sci Lett 338:L869
40. Saliba N, Parker DH, Koel BE (1998) Surf Sci 410:270
41. Sueyoshi T, Sasaki T, Iwasawa Y (1995) Surf Sci 343:1
42. Sueyoshi T, Sasaki T, Iwasawa Y (1996) Surf Sci 365:310
43. Burghaus U, Conrad H (1996) Surf Sci 352:253
44. Burghaus U, Vattuone L, Gambardella P, Rocca M (1997) Surf Sci 374:1
45. Barth JV, Zambelli T (2002) Surf Sci 513:359
46. Mguig B, Calatayud M, Minot C (2004) Theochem 709:73
47. Pillay D, Hwang GS (2006) J Chem Phys 125:144706/1
48. Wu X, Selloni A, Nayak SK (2004) J Chem Phys 120:4512
49. Lee S, Fan C, Wu T, Anderson SL (2004) J Am Chem Soc 126:5682